Refinement and Biofidelity Evaluation of the THUMS Small Female Ankle.

Ramakrishnan Balaji Iyer, Adrian Felix Caudillo-Huerta, Bronislaw Gepner, Jason Hallman, Matthew B. Panzer, Jason L. Forman

Abstract Ankle injury prediction in motor vehicle crashes poses challenges due to the chaotic nature of ankle loading and the breadth of loading modes possible. The study seeks to refine the ankle joints in the THUMS v4.1 small female model and compare the biofidelity of the model against available Post-Mortem Human Subjects (PMHS) data. First, cartilage was added using hexahedral elements on the articulating surfaces to fill any voids between the bones and to improve continuity of load transfer. Next, a Mil-Spec shoe model was fitted to the foot by a systematic process. The refined and updated model was evaluated by performing four biofidelity validation cases - compressive axial impact, dorsiflexion, inversion, and eversion - replicating experiments conducted on small female PMHS with the same shoes. Also, a sensitivity analysis was performed on the material model of the ankle ligaments to understand the effect on the model response. The refined model showed consistency with the PMHS test results over the suite of validation cases performed. From the results, it was observed that the interaction between the bones has improved with the addition of cartilage resulting in softer response due to reduced rigid contacts. The addition of the shoe also enhanced the realistic simulation of ankle loading in likely real-world scenarios.

Keywords Ankle biofidelity evaluation, 5th percentile female, THUMS, Finite Element Human Body Model, Shoe fitting.

I. INTRODUCTION

Ankle fractures are one of the more frequent types of AIS2+ injuries among the belted automobile occupants involved in frontal collisions. Ankle injuries also have been reported to represent one of the greatest differences in AIS2+ injury risk between females and males in frontal automobile collisions. Specifically, analyses of field data indicate that females face a higher risk of ankle fractures compared to males even after accounting for age, height, BMI, and delta-V. However, the underlying cause of this disparity in risk remains unclear [1]. The ankle remains one of the most challenging body regions to predict injury risk, given the breadth and complexity of loading possible. Human body models (HBMs) may aid in ankle injury prediction with the potential for tissue-level injury prediction under a variety of loading modes.

Computational HBMs are an increasingly important research tool and may complement physical safety assessments in the future. HBMs must be sufficiently accurate in terms of their anatomy and biofidelity to accurately predict injury risk under complex loading modes. Consequently, validating HBMs helps to ensure that the model response shows a reliable representation of a human body response. Validations of HBMs are carried out at various levels, including local tissues, organs, bones, joints, and full body, often compared against the Post-Mortem Human Subjects (PMHS) experimental data. The THUMS (Total Human Model for Safety) F05 v.4.1 is one such HBM that has been developed with a high level of detail. This HBM incorporates intricate anatomical structures and has been validated for various body regions, such as the head, neck, chest, abdomen, pelvis, and extremities [2]. Given the wide variety of ways that the ankle can be loaded and injured even in a frontal collision [3], it is important to refine and evaluate the biofidelity of HBM ankles under different loading modes.

In the THUMS F05 v.4.1, the foot and ankle region consist of the distal ends of the tibia, fibula, and talus, and calcaneus bones, interconnected by ligaments. However, in the baseline model's foot and ankle, there are gaps measuring 4–5mm between the ankle bones. The foot has up to now lacked representation of shoes, and testing

R. B. Iyer (+1-434-257-3722, zdf5ks@virginia.edu) and A. Caudilo are Research Engineer, B. Gepner is a Senior Scientist, M. Panzer is an Associate Professor and J. Forman is a Research Associate Professor at Center for Applied Biomechanics at University of Virginia, USA. J. Hallman is a Senior Manager at Collaborative Safety Research Center, Toyota Motor North America

has shown that the presence of shoes can affect ankle kinematics and injury responses [4]. Given that occupants typically wear shoes in vehicles, it is desirable to integrate a shoe model into the HBM for accurate prediction of ankle injuries in automotive loading scenarios.

The goal of this study was to refine the foot and ankle region of the THUMS F05 v.4.1 to enhance its anatomical representation and biofidelity. The refinement includes addition of cartilage on the articulating surfaces, as well as integration of a shoe with a fitting process designed to achieve a snug fit around the foot. The updated model with cartilage and shoes was evaluated against testing conducted on 5th percentile female PMHS with shoes under four ankle loading scenarios: compressive axial impact, dorsiflexion, inversion, and eversion. Also, a sensitivity study was performed on the material model of the ankle ligaments to investigate their role on load sharing within the ankle model.

II. METHODS

Cartilage Modeling

The first refinement step consisted of incorporating the ankle cartilage into the model. Cartilage has an important biomechanical role as it provides a continuous surface of engagement, modulating hard contact and smooth load transfer between the bones, and ensuring proper loading of the soft tissues of the ankle [4]. Cartilage was added to the paired articulating surfaces of four joints within the ankle: the tibio-talar joint, the tibio-fibular joint, the fibulo-talar joint, the subtalar joint (between the talus and the calcaneus). For each of these joints, cartilage was modeled by performing a solid offset/extrusion of the mesh present on each opposing face of the joint. The offset was performed with a uniform thickness seeking to fill the existing gap between the bones. The mesh was then manually morphed to remove penetration. The elements in the mid-substance of the cartilage generally consisted of hexahedral elements. The elements at the periphery of the cartilage were converted to tetrahedral or pentahedral elements to smooth the transition to the bone (Fig. 2). Figure 1 shows the THUMS F05 comparison between the ankle bone gaps before (Fig. 1a) and after (Fig. 1b) addition of the cartilage. As the cartilage is much softer than bone, the material model assigned for these cartilages is **MAT_ELASTIC* with the density of 2.0E-06 kg/mm^3 and youngs (E) modulus of 200 MPa [5].

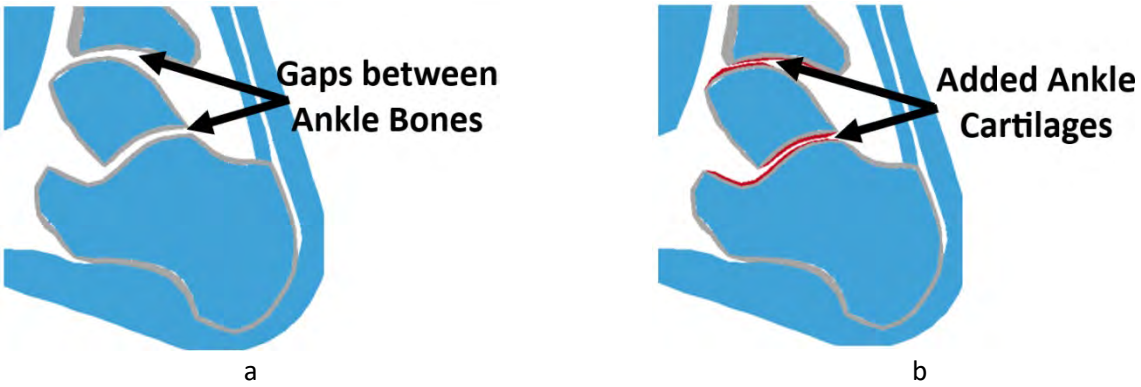

Fig. 1. Cross section of the THUMS F05 ankle a) before b) after addition of the cartilage added to the various articular surfaces of the ankle (highlighted in red color).

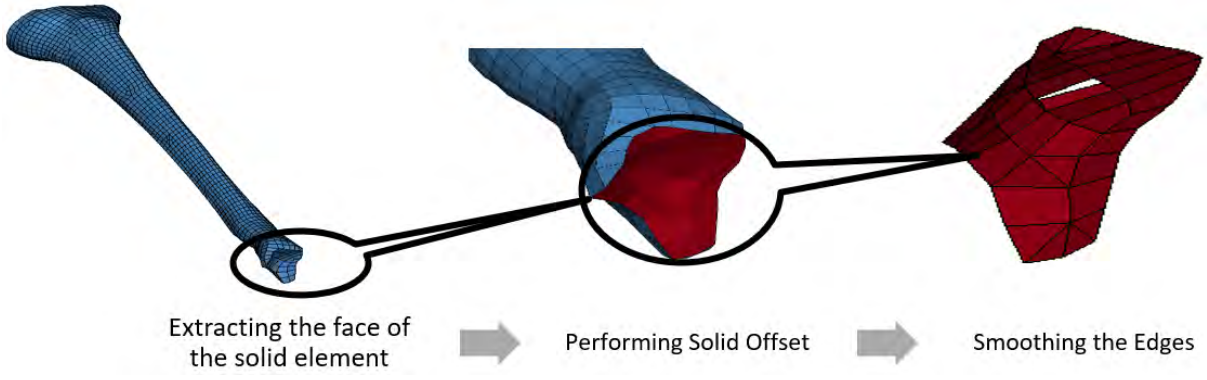

Fig. 2. Illustration for the process for generating the ankle cartilage

Integration of Shoe in THUMS 5th Percentile Female Occupants

While previous studies indicated that while the presence of a shoe does not necessarily change the injury tolerance of the ankle, it can change the nature of the kinematics and loads applied to the ankle (by changing the coupling and stiffness of the forefoot) [4]. For realistic ankle loading and interaction with the surrounding environment, it is helpful to include a representation of a shoe for use with human body models. Therefore, a shoe was fitted to the THUMS v.4.1 5th percentile female model as a part of the ankle model refinement. The geometry of this shoe was based on a 3D scan of a standard Mil-Spec shoe (MIL-S-21711E) commonly used with the Hybrid III 5th percentile female dummy. The fitting process for the shoe was inspired by similar past efforts [5], with substantial changes in the process to attempt to optimize the fit for the THUMS.

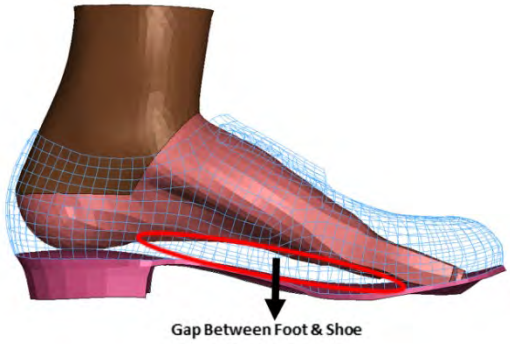

a) Preliminary Shoe Fitting

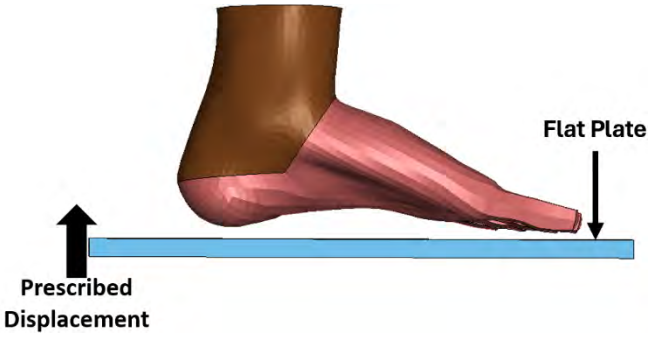

b) Foot Flattening Simulation Setup

c) Flattened Foot

Fig. 3. a) Preliminary shoe fitting, keeping the initial posture of the foot static. b) Simulation setup for flattening the foot. c) Flattened foot by pressing the flat plate.

The overall goal was realistic coupling between the shoe and the foot, to minimize slippage between the two when subjected to dynamic load. The fitting process involved a series of 4 simulations: shrinking/expansion of foot and ankle, contraction of shoe, folding of lace flaps, and tightening of the laces (represented by 1D seatbelt elements). To reduce the computational time, the foot and ankle (including distal tibia and fibula bone) were isolated from the HBM during shoe fitting process. Upon preliminary shoe fitting to THUMS F05 foot, it was observed that significant gaps persisted between the foot and the inner surface of the shoe due to the initial posture of the foot (Fig. 3.a). To reduce the initial gaps, pre-simulation was performed by pressing the flat plate against the foot to flatten the arch (Fig. 4.b and Fig. 3.c).

Once the arch was flattened, the foot and ankle were manually scaled down to smaller sizes ensuring no penetration with shoe (as shown in Fig. 4.a). Contact was defined between the foot skin and shoe, and the foot was expanded to its original size via simulation. During this first stage, the shoe naturally assumed the primary orientation of the foot as it was not constrained (Fig. 4.b). Once the primary shape was taken by the shoe, the next stage was to shrink the shoe via thermal contraction to adjust the size of the shoe to match the foot, and to reduce gaps between the shoe and the foot. A thermal contraction simulation was conducted on the shoe with the foot and ankle kept rigid, leading to a reduction in internal gaps. As a result, the profile of the shoe closely resembled that of the foot and ankle (Fig. 4.c). Subsequently, in the next stage lace flaps were folded and the laces (represented as 1D seatbelt elements) were tightened using pretensioner elements (Fig. 4.d and Fig. 4.e). During the entire process of shoe fitting, the ankle and the foot bones were considered rigid without any spatial constraints other than the constraint provided by the connecting ligaments and flesh. The final shoe model along with the modified foot and ankle geometry was then integrated to the THUMS F05 v4.1 model (Fig. 4.f).

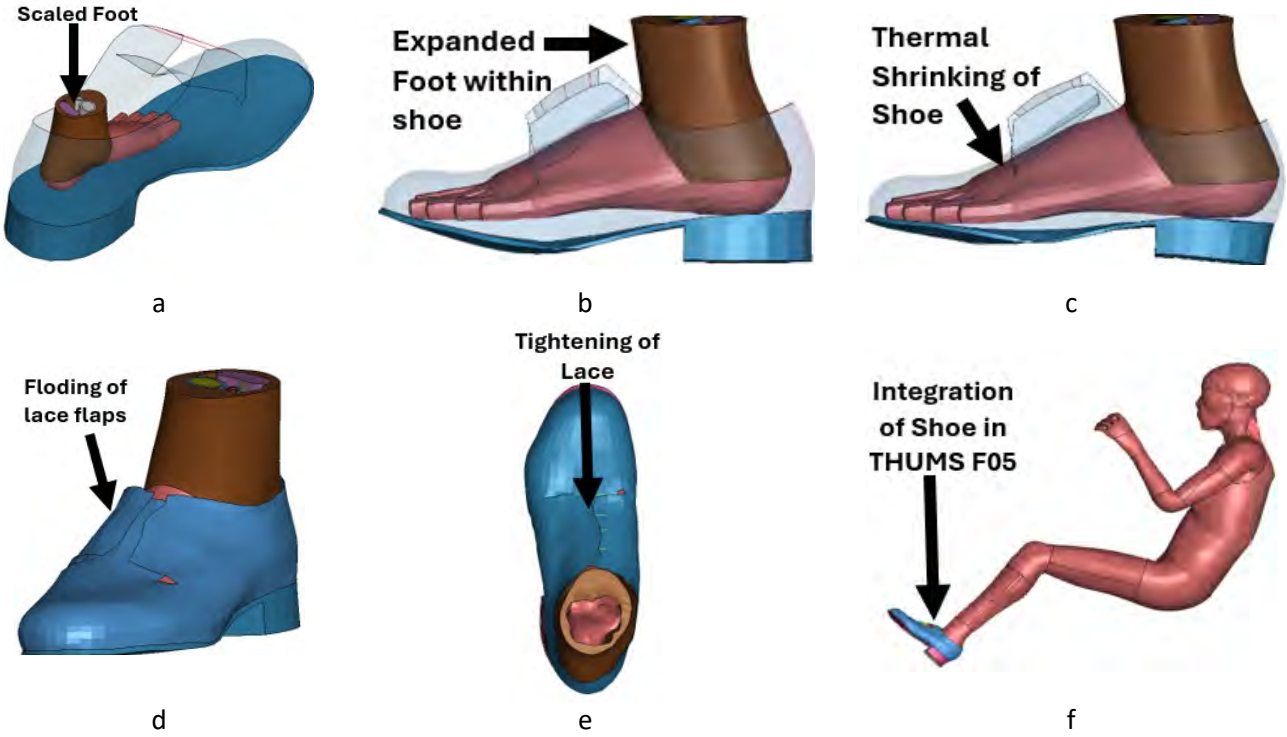

Fig. 4. Shoe fitting process: a) shrinking and b) expansion of foot and ankle within the shoe c) thermal contraction of the shoe around the foot d) folding of lace flaps e) tightening of laces f) integration of shoe in THUMS F05 v4.1. Note that the entire foot and ankle were kept rigid for only one particular step of the shoe fitting process (thermal contraction). For the rest of the shoe fitting process, only the bones were defined as a rigid (without any spatial constraints other than the ligaments connecting the bones) and other parts were allowed to deform.

Ankle Biofidelity Evaluation for THUMS F05

For evaluation of biofidelity of the F05 foot and ankle model, validation cases were chosen for which PMHS test data were available and which represent loading scenarios that are likely to contribute to injury in automobile collisions. Priority was placed on identifying load cases. The load cases selected include whole-ankle tests involving compressive axial impact to the underside of the foot [6], dorsiflexion of the ankle [7], and inversion/eversion of the ankle [8]. These tests all were performed specifically on small female PMHS (as opposed to scaling from tests on mid-sized males), and all were performed both with and without shoes. For the simulation, Bone or ligament material failure was not considered.

Axial Impact

Reference [6] developed biofidelity corridors from axial impact tests performed on lower extremity component specimens from small female PMHS (five tests without shoes, six tests with shoes). In these tests, the lower leg (from mid-thigh) of PMHS was isolated and supported within a rigid support structure, and impact was applied to the plantar surface of the foot via a rigid flat impactor. The impactor consisted of a 28.4 kg mass moving along a guided rail, with an impact velocity of approximately 2.9 m/s.

This test setup was recreated in simulation by separating the lower limb (from mid-thigh) of the updated THUMS F05 and constraining the motion of the femur in all degrees of freedom (DOF). Two model setups were developed for each update carried out in the THUMS F05: i) after addition of ankle articular cartilage (without shoe) and ii) after integrating of shoe. The shoe sole (or the foot in case of without shoe) was rested against an impactor footplate, and an impactor was driven by a prescribed motion displacement-time history based on the impactor motion recorded in the tests (with the impactor in contact with the plantar surface of the shoe/foot). The model setup for the THUMS F05 with shoe is shown in Fig. 5.a. Forces were measured in the mid-tibia and were plotted against the displacement of the impactor to compare with the experiment results. (Note: This biofidelity evaluation – axial impact – was chosen prior to shoe fitting to assess the model stability with ankle cartilage in case of maximum ankle bone interaction).

Dorsiflexion

Reference [7] developed biofidelity corridors from dynamic dorsiflexion tests performed on lower extremity component specimens from small female PMHS (six tests without shoes, seven tests with shoes). The test setup

was the same as the one used in the axial impact test with only one change. Here, the ball of the foot was impacted via a rigid cylindrical impactor (instead of impacting the whole bottom of the foot with a flat plate), with an impact velocity of approximately 3.0 m/s.

For the FE simulation, the same setup file was used which was created for the axial impact and the flat impactor was replaced by a rigid simulated cylindrical impactor (Fig. 5.b). The impactor was driven via prescribed motion, defining the motion time-history based on the average impactor motion time-history measured during the tests. Outputs included the change in dorsiflexion angle of the ankle (defined based on the angle of the calcaneus, measured via Vicon motion capture in the experiments) compared to the cross-sectional moment in the ankle. The ankle moment was calculated by measuring the force and moment in a cross-section of the tibia and translating via rigid body transformation to the ankle joint center. This is similar to the methods used in the experiments, where the cross-sectional tibia and fibular forces were measured via implanted load cells and then translated to calculate the moment in the ankle.

Inversion/Eversion

Reference [8] conducted dynamic inversion and eversion tests performed on lower extremity component specimens from small female PMHS (five tests without shoes, five tests with shoes). In these tests, the proximal tibia was fixed within a rigid potting device, and a 2 kN axial preload was applied to pre-compress the ankle. The ankle was then rotated in inversion or eversion via rotation of a flat rigid plate pressed against the bottom of the foot (with some lateral supports in place to improve coupling of the foot to the plate). Ankle rotation was measured directly via an array of Vicon motion tracking markers installed on the calcaneus. Moment in the ankle was calculated by transforming moments and forces measured with external load cells to the ankle joint centre via rigid body transformation.

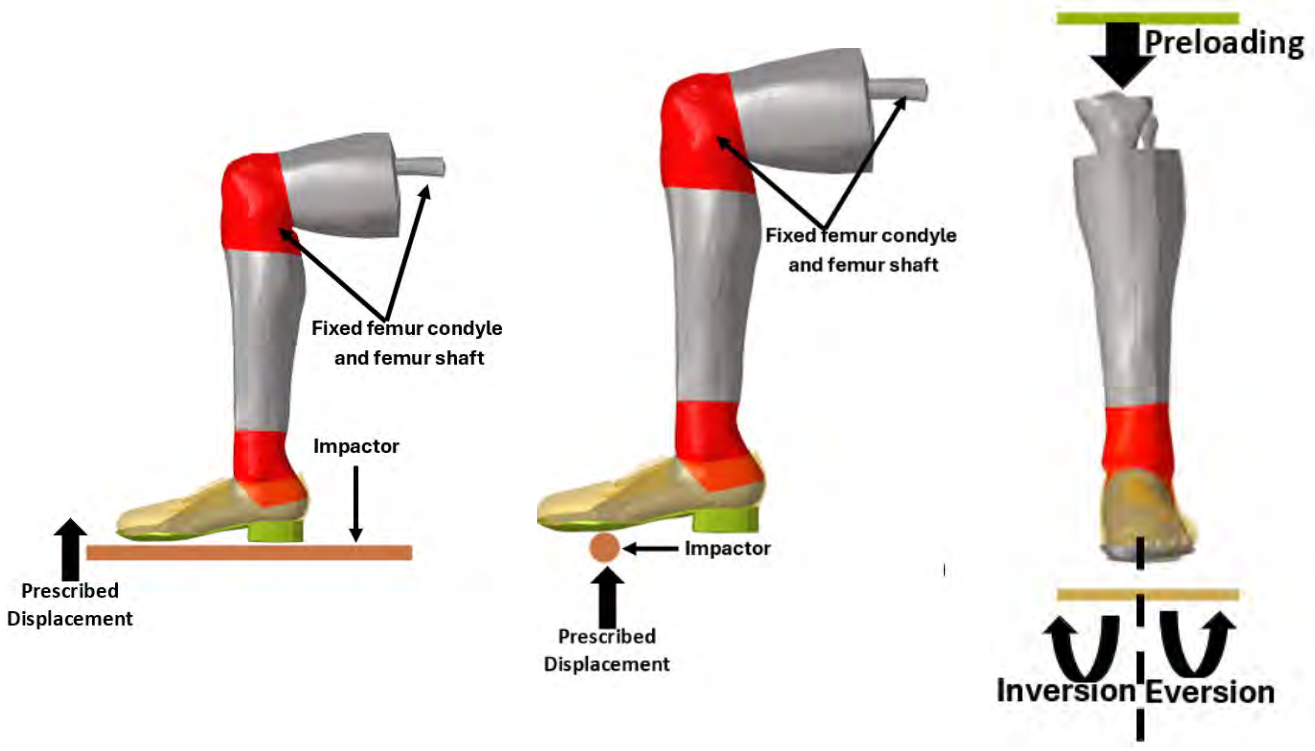

a b c

Fig. 5. Simulation setups of ankle biofidelity validation cases: a) axial impact b) dorsiflexion impact c) inversion and eversion.

These tests were simulated by constraining the motion of the proximal tibia using a rigid plate at the top of the tibia. The leg was preloaded by applying static 2 kN axial force to the top plate and this load was confirmed using the cross-section force-time history measured in the mid-tibia shaft as in the experiment (Fig. 5.c). The shoe sole was rigidly fixed to the bottom plate in all DOF, and then rotation was applied to the plate via prescribed motion (based on the average plate rotation time-history measured in the tests. The moment occurring in the ankle was calculated via the same instrumentation and transformation method described for the dorsiflexion simulations above.

THUMS F05 Instrumentation

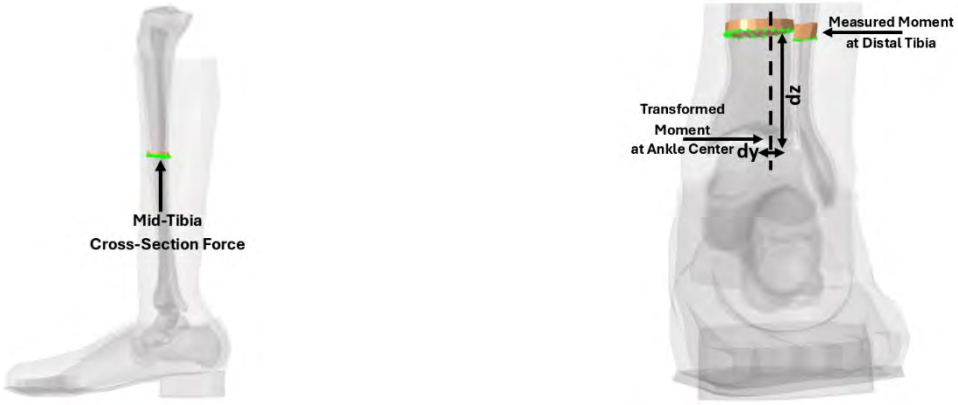

a b

Fig. 6. Model instrumentation a) cross-section force at mid-tibia b) the moment at the ankle joint center calculated via transformation of the forces and moments measured in the distal tibia and fibula.

Output such as the forces and moments were recorded during the simulations to compare against the experimental results. The output forces and moments were measured by defining cross-section areas at the mid and distal tibia (Fig. 6.a). The resultant moment at ankle center was computed by performing rigid body moment transformation of the forces and moments measured at the distal tibia (Fig. 6.b).

Sensitivity Study of the Ankle Ligaments' Material Model

In the current THUMS F05 v4.1, seven ankle ligaments are present which are modeled as 2-D shell elements formulated as **MAT_FABRIC*. Four out of the seven ligaments are on the medial side of the model connecting the tibia bone to the talus bone and the rest of them are on the lateral side connecting the fibula bone to talus and calcaneus bone. These ligaments are shown in Fig. 7. Preliminary simulations in inversion and eversion showed that in both loading modes the ligament force response tended to be dominated by the talo-tibular anterior ligament in the early portion of the simulation (Fig. 8). To investigate this further, we sought to perform a sensitivity analysis on the ligament material model to see if it is possible to implement a formulation that results in a more even distribution of load among the ligaments, without adversely affecting the overall biofidelity.

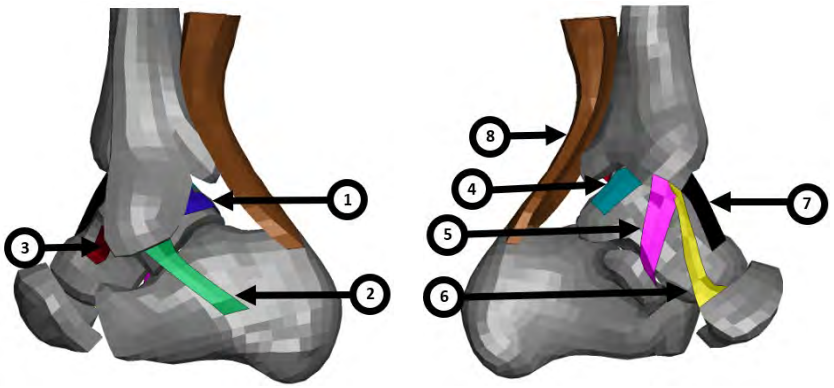

Nr.	Ligament Name
1	TALOFIBULARE_POSTERUS
2	Calcanofibulare
3	TALOFIBULARE_ANTERIOR
4	TALOTIBIULARE_POST
5	TALOTIBULARE_MED_1
6	TALOTIBULARE_MED_2
7	TALOTIBULARE_ANT
8	ACHILLES_TENDON

a b c

Fig. 7. THUMS F05 v.1 Ankle ligaments a) lateral b) medial c) nomenclature of the ligaments

Given the dominance of the anterior talo-tibular ligament, the sensitivity analysis began with modifying the material model of this particular ligament. From the experiments conducted by [4] focused on ankle ligaments, it was observed that ligament force-displacement behavior tends to exhibit a hyperelastic response. Therefore, the material model was changed from fabric to hyperelastic material model viz. **MAT_OGDEN_RUBBER*. The values of the material constants (μ and α with shear modulus G of 85 MPa) were derived using the force-displacement curve of anterior tibiotalar plotted in [9]. As a starting point, the same material model was applied to all other remaining ankle ligaments. Then the Ogden rubber material properties were modified, targeting adequate performance in the inversion/eversion response relative to the target corridors (either matching or improving upon the results with the original material formulation). After refining these material model coefficients by iteratively modifying, the inversion/eversion cases were re-run for a final assessment.

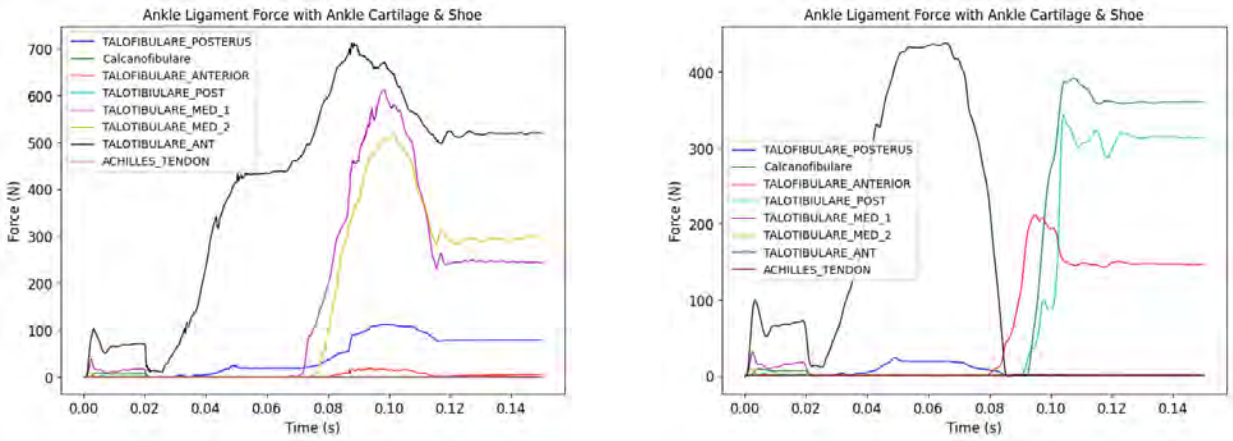

a) Eversion b) Inversion

Fig. 8. Resultant Cross-sectional forces of the ankle ligaments obtained from a) an eversion simulation, and b) inversion.

III. RESULTS

Results obtained from the axial impact validation simulation performed for THUMS F05 after addition of ankle cartilage was compared with the simulation result of the THUMS F05 baseline and with the PMHS biofidelity corridors developed from small female tests result without shoes as shown in Fig.9 [6]. The peak force for the THUMS F05 baseline model and for the THUMS F05 with ankle cartilage are approx. 3900 N and the 3500 N respectively.

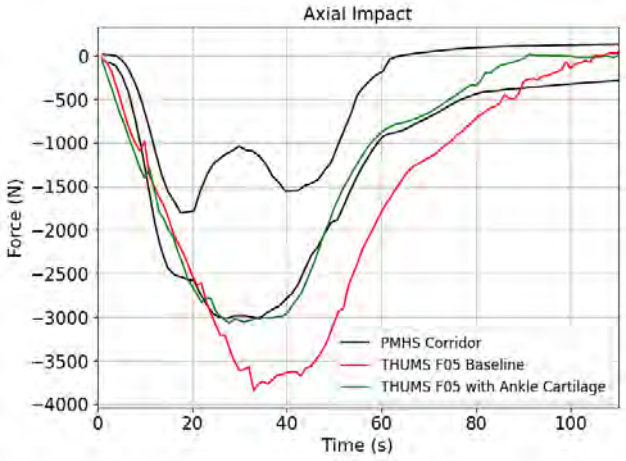

Fig. 9. Cross-sectional tibia force from the axial impact simulations, comparing THUMS F05 with ankle cartilage (green) to THUMS F05 Baseline (i.e. without ankle cartilage) (red) and the PMHS corridor (black).

Simulation results of the ankle biofidelity validation cases for THUMS F05 with the shoe were compared to respective PMHS biofidelity corridors produced from small female tests with shoes. Also, the regions of peak strain obtained from the simulation were compared to the injuries recorded during the experiments. These peak strain regions were identified by considering a threshold of 2% of maximum plastic strain for the cortical bones.

For axial impact validation, the shoe was rested on the impactor with a minimal gap to avoid numerical error. As discussed in the pervious section, mid-tibia cross section force time-history was recorded. This force was plotted against the displacement and was compared with the force-displacement PMHS corridor as shown in Fig. 10. The model reached a maximum force of 3000N when the impactor was displaced 22mm. Overall, the response was within the PMHS corridors until 18mm of impactor displacement after which the model had a somewhat stiffer response in comparison to the experiments, but the overall Correlation Analysis (CORA) score was 0.9887. There were peak strain regions observed at the tibia plateau and distal tibia. Similar observations were also found in the experiments, where fracture was also identified at the tibia plateau and distal tibia.

The dorsiflexion validation was performed using a rigid cylindrical impactor and the moment at ankle center is reported and plotted against the change in shoe angle. The moment at ankle center was calculated by rigid body transformation of the moment at the distal tibia. The foot angle time-history was measured by considering the change in the angle of the front shoe with respect to the shoe-heel. The comparison of the moment versus

shoe angle plot between the PMHS corridor and the THUMS F05 model is shown in Fig. 11. The simulation results are in agreement with the experimental results and the CORA score was 0.9830. For 30° of shoe rotation, there was 30 Nm of moment generated at the ankle center. No fracture was observed in the experiment, and no bone elements exceeding 2% plastic strain were observed in the simulation.

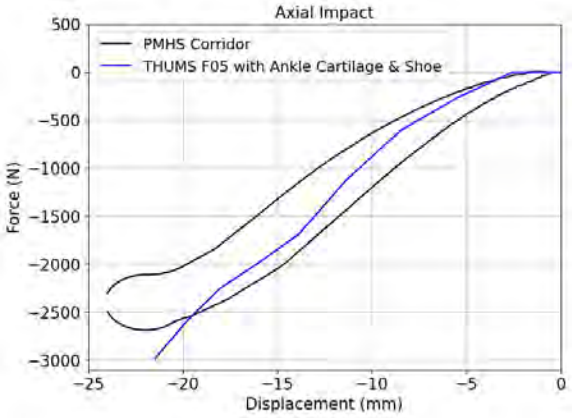

Fig. 10. Cross-sectional tibia force from the axial impact simulations, comparing the updated THUMS F05 with ankle cartilage and shoe (blue) to the PMHS corridor (black).

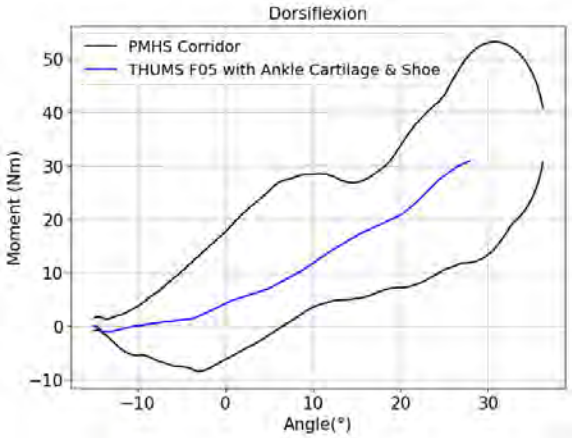

Fig. 11. Transformed ankle moment from the dorsiflexion simulations, comparing the updated THUMS F05 with ankle cartilage and shoe (Blue) to the PMHS corridor (black).

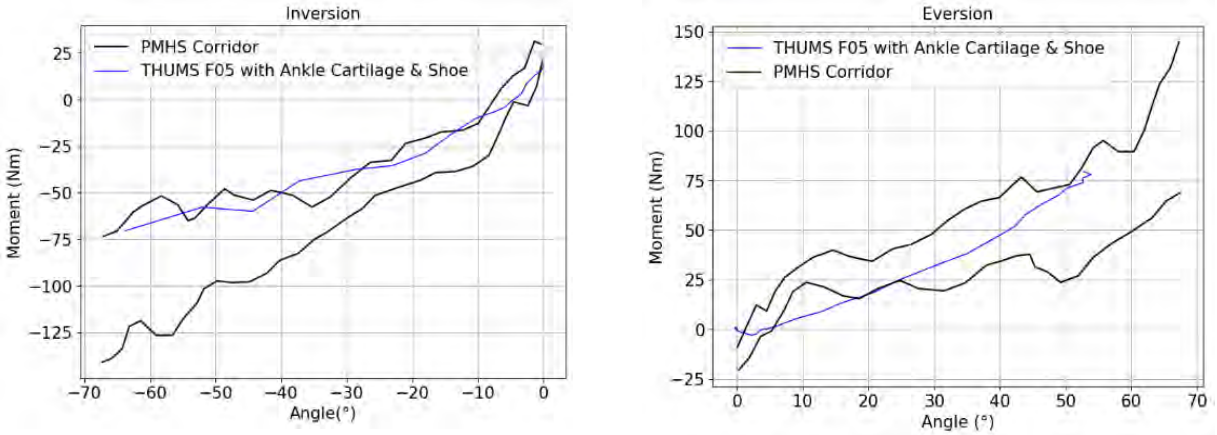

a b

Fig. 12. Ankle moment from the a) inversion b) eversion simulations versus the rotation angle of the calcaneus, comparing the updated THUMS F05 with ankle cartilage and shoe (blue) to the PMHS corridor (black).

For the inversion and eversion, the ankle moment versus the rotation angle of calcaneus was plotted and compared to the PMHS corridor developed by reference [10]. The simulation results obtained for the inversion and eversion validation cases are shown in Fig. 12. The ankle moment was computed by performing the rigid body transformation of the distal tibia moments similar to the dorsiflexion validation case. Here, the rotation angle of calcaneus was measured with respect to the tibia bone as it was measured in the experiment. In the inversion validation case, THUMS F05 with shoe showed a softer response and fell on the lower bound of the PMHS corridor and the CORA score was 0.8445. The maximum moment was 60Nmm at 63° of calcaneus rotation. In the eversion validation case, THUMS F05 with shoe behaves soft for initial 15° of calcaneus rotation, after which it shows a stiffer response. Overall, the response was within the PMHS corridor, and the CORA score was 0.9365. Also, the regions of peak strain observed in both the simulation results were consistent with fractures observed in experiments.

Comparison of FE Model Results with PMHS Injuries

The peak strain regions observed in the simulations were compared to the injury types observed in the PMHS tests to get a general idea of whether they are consistent. Strain peaks were defined as regions where the effective plastic strain exceeded 0.02. As can be observed in Table 1 below, the locations of the strain hotspots

were generally consistent with the injury types observed in the tests. The snapshots used here are taken during the last time step and the red color elements are ones that registered an effective plastic strain of 0.02.

Table 1
COMPARISON OF FE STRAIN HOTSPOTS RESULTS WITH EXPERIMENTAL FRACTURE

Loadcase	Experimental Fracture Location Injury	FE simulation strain hotspot location	Image
Axial Impact	Tibia plateau fracture, distal tibia fracture [6]	Tibia plateau, distal tibia and fibula	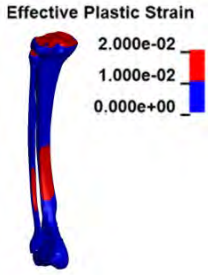
Dorsiflexion	No fracture [7]	No regions exceeding 2% plastic strain	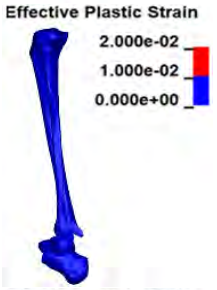
Inversion	Calcaneofibular (CF) avulsion, medial malleolus fracture [8]	Distal tibia and fibula, medial malleolus	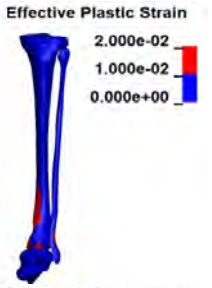
Eversion	Medial malleolus fracture, distal tibia fracture, deltoid rupture [8]	Medial and lateral malleolus, distal tibia and fibula, talus	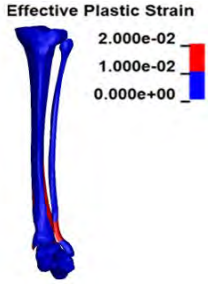

Refinement of Ankle Ligament's Material Model

The updated material models for the ankle ligaments were evaluated for two load cases (inversion and eversion) as discussed previously. The simulations ended with a normal termination confirming the stability of the new ankle ligament material for the given loading conditions. The results obtained from these simulations are shown in Fig. 13. In the case of inversion, the baseline and modified material models result in similar moment-angle stiffness to approximately 45 degrees of ankle rotation, beyond which the modified model exhibits a somewhat softer response. Similarly, for eversion the baseline and modified material models result in similar moment-angle stiffness to approximately 35 degrees of ankle rotation, beyond which the modified model exhibits a softer response.

The resultant cross-sectional forces of the ligaments were compared for both models against the respective loading conditions, shown in Fig. 14 and Fig. 15 for eversion and inversion respectively. In the eversion loading case, it was noted that the anterior tibiotalar ligament registered a maximum resultant cross-section force of approximately 250N, which is 550N lower compared to the default ankle ligament material model. Similar reductions in peak forces were observed in the other two medial ligaments. These decreases in peak forces were consistent with the findings from the inversion loading case. In addition to evaluating the ligament cross-sectional

forces, the elongation of the ligaments was also measured at the end of the simulation for both the loading case and was compared to the simulations with the default material. It was found that the ligaments with updated material exhibited approximately 10mm more elongation than those with the default material.

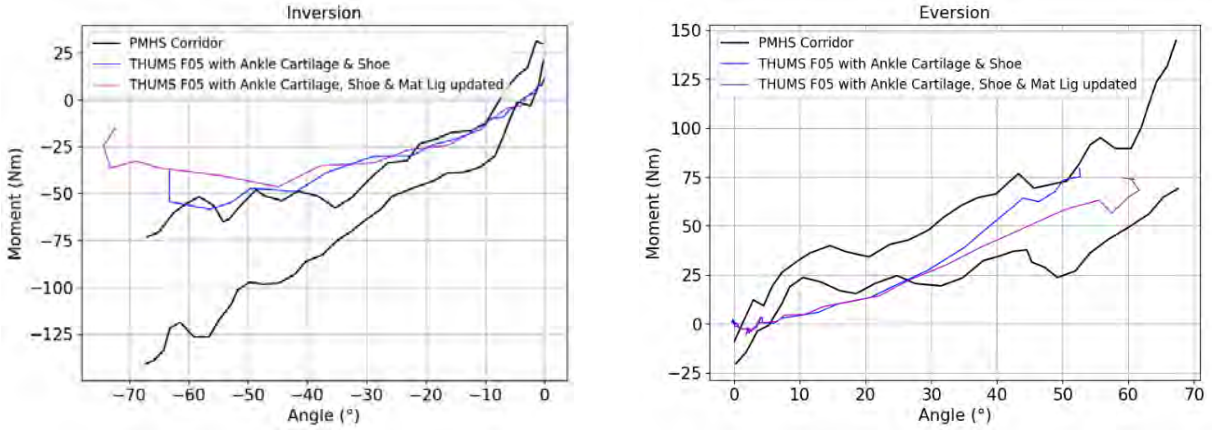

a) Inversion b) Eversion

Fig. 13. Resultant cross-sectional forces of the ankle ligaments obtained from: a) Inversion and b) Eversion simulations with the updated material model.

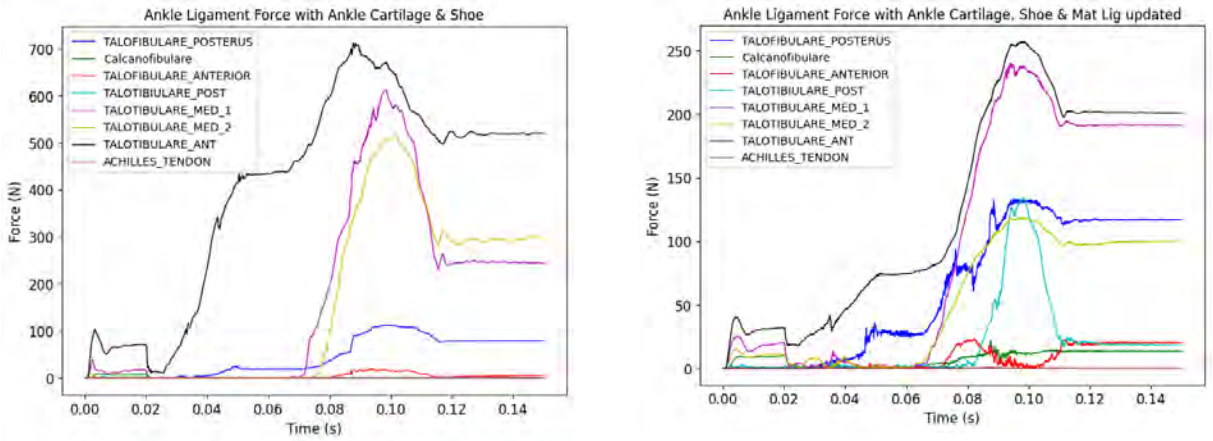

a) Default ankle ligament material b) Updated ankle ligament Material

Fig. 14. Resultant cross-sectional forces of the ankle ligaments obtained from eversion simulations; a) default and b) updated ankle ligament material.

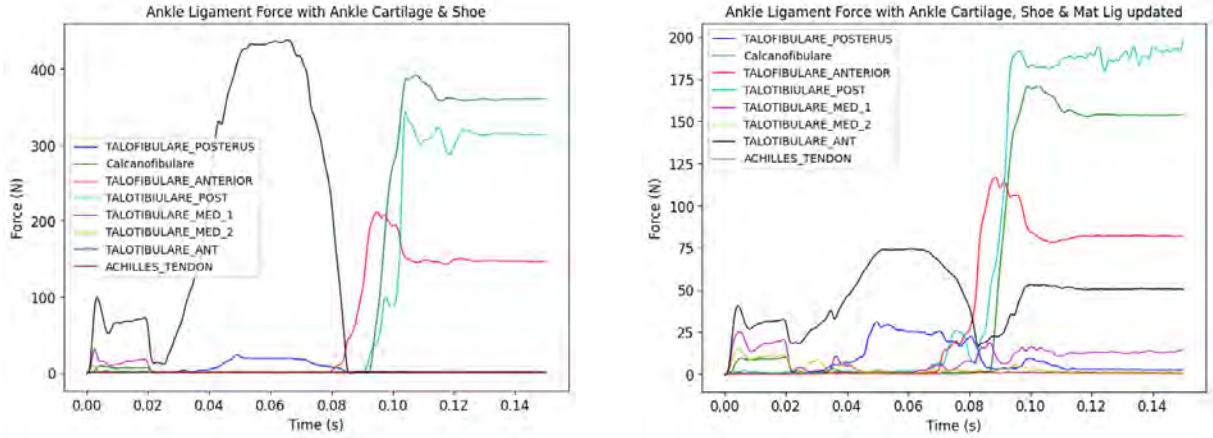

a) Default ankle ligament material b) Updated ankle ligament Material

Fig. 15. Resultant Cross-sectional forces of the ankle ligaments obtained from inversion simulations; a) default and b) updated ankle ligament material.

IV. DISCUSSION

Ankle fractures remain common injuries in automobile collisions, with field data indicating a higher risk among females compared to males. However, the underlying cause of this sex-based difference remains unclear. Computational HBMs may be utilized to investigate the factors contributing to higher female ankle injury risk and

develop future prevention strategies. To facilitate this, an HBM with accurate ankle biofidelity is necessary to accurately predict ankle injury. This study enhanced the anatomical representation of the foot and ankle region of the THUMS F05 model by adding ankle cartilage and integrating a shoe commonly used in automobile safety evaluations. Comparisons of results, including forces and ankle moments, against experiments conducted on small female Post-Mortem Human Subjects (PMHS) with shoes revealed overall agreement with PMHS corridors. The addition of cartilage helped fill voids between bones and improve load transfer continuity, confirmed through comparing the axial impact biofidelity evaluation simulations results for THUMS F05 baseline and with cartilage models (fig. 9).

For the THUMS F05 with ankle cartilage and shoe, during the axial impact biofidelity validation, the model's response remained within the PMHS corridor until the impactor displacement reached 20mm, after which the model displayed a stiffer response. For dorsiflexion, the model results fell within the lower and upper bounds of PMHS. In inversion and eversion loading, while the model exhibited slightly stiff and soft responses, respectively, the overall responses reasonably matched the corridors. Comparison of peak strain regions to injuries observed in the PMHS testing revealed similar patterns, suggesting that the model captures at least some aspects of the internal distribution of load experienced in these load cases.

The material model of the ankle ligaments was modified by changing the material model from fabric to hyperelastic (Ogden Rubber material model) to study the effect on the responses in the inversion and eversion loading modes. The updated material model showed a slightly softer response in comparison to the default material model. Also, the ankle biofidelity was improved for the updated material model as the range of motion (rotation of calcaneus) increased by about 10° in both loading modes. Overall, the responses remained generally consistent with the PMHS corridors, fitting the eversion corridor better than the inversion corridor. Greater load sharing among the ankle ligaments was observed from the distribution of ligament cross sectional forces (Fig. 14 and Fig. 15). The new material model tended to decrease the dominance of the anterior tibiotalar ligament. This is generally consistent with the updated material exhibiting a softer response, allowing 10mm more elongation of the anterior tibiotalar ligament which then increases the load sharing to other surrounding ligaments. It is challenging to discern if redistribution of load to other ligaments represents an improvement in biofidelity, as the load sharing between ankle ligaments has not been observed directly in PMHS tests. In the available inversion/eversion PMHS tests, a variety of different injury patterns were observed in different bony and ligament locations. This observation supports a hypothesis that the resisting force is not borne solely by the ATFL [8]. At a minimum, this exercise demonstrates that it is possible to modify the internal distribution of load by modifying ankle ligament stiffnesses without adversely affecting the gross moment-angle biofidelity of the model. This process could be continued by refining the material model of each individual ligament if new experimental data becomes available.

This study is an advancement in the continuing development and refinement of research tools to aid in ankle injury prediction and prevention in automobile collisions. The enhanced THUMS F05 ankle model demonstrated predictions of peak strain regions consistent with injury locations observed in matched tests. With this level of fidelity established, the model may serve as a foundation to consider the variability in local injury tolerance and ankle bone geometry observed in the population. In parallel efforts, we have experimentally quantified the local injury tolerance of the distal tibia and fibula via PMHS tests with isolated bones [11]. We recommend that future work include further investigation into variations in fracture tolerance or anatomy to evaluate and refine the HBM's ability to predict tissue-level ankle fracture risk, and to capture the effects of variations in ankle bone geometry in the population.

Limitations

The shoe fitting method in this study was developed iteratively and includes a few pragmatic choices. First, the pre-simulation step flattened the arch to reduce gaps between the foot and the inner surface of the shoe that persisted due to the initial posture of the foot (Fig. 3.a). Although this step altered the alignment between the phalange and tarsal bones. Additionally, a uniform coefficient of thermal expansion was used during the thermal simulation to reduce the gap between the shoe and the foot. The result of this thermal expansion may be affected somewhat by the shoe material properties which vary in different parts of the shoe. These different material properties responded differently to thermal changes and may not uniformly reduce gaps due to uneven contraction. While the overall methodology can be followed for applying other shoes to other FE-HBMs, the authors would encourage more research into such practices to improve the process where it is warranted. Lastly,

much of this study focused specifically on the ankle, adding cartilage and modifying ligaments between the ankle bones. The authors therefore also would encourage extending these sorts of refinements to the bones of the midfoot in future work.

V. CONCLUSION

Ankle fractures remain one of the most common AIS2+ injury types in automobile collisions and may occur through a complex variety of loading modes. In this study the foot and ankle model of the THUMS v.4.1 5th percentile female was refined to improve its anatomical fidelity (including addition of cartilage), its biofidelity, and addition of fitted models of shoes. First, cartilage was added to the paired articulating surfaces of four joints within the ankle. Then, a shoe model was fitted to the THUMS foot by a multi-step process involving shrinking/expanding the foot within the shoe, wrapping the shoe around the foot, and lace-tightening to achieve a snug fit. The updated model was evaluated by performing four biofidelity validation cases - compressive axial impact, dorsiflexion, inversion, and eversion - replicating experiments conducted on small female PMHS with the same types of shoes. The refined model showed consistency with the PMHS test results for all the cases, including the location of peak strain regions compared to fractures observed in the tests. Lastly, the material model of ankle ligaments was updated, leading to a more even distribution in the load shared across the ligaments within the ankle. With these refinements, this model may now serve as a foundation to further investigate ankle injury mechanisms in simulated automobile collisions.

VI. ACKNOWLEDGEMENTS

This work was funded by the Toyota Collaborative Safety Research Center (CSRC). The authors also acknowledge Research Computing at The University of Virginia for providing access to computational resources and technical support that have contributed to the results reported within this publication.

VII. REFERENCES

[1] Forman, J., Poplin, G. S., Shaw, C. G., McMurry, T. L., Schmidt, K., Ash, J., Sunnevang, C. (2019) Automobile injury trends in the contemporary fleet: Belted occupants in frontal collisions. Traffic injury prevention, **20**(6): pp.607–12.

[2] Toyota Motor Corporation (2021), Toyota Center R&D Labs., INC. Total human model for safety (THUMS) user's manual, AF05 Occupant Model Version 4.1.

[3] Funk, J.R. (2011), Ankle injury mechanisms: Lessons learned from cadaveric studies. Clin. Anat., 24: 350-361. https://doi.org/10.1002/ca.21112

[4] Roberts, C. W., Kerrigan, J. R., Forman, J. L. (2017) Shod and unshod kinematic response of the female lower extremity under dorsiflexion loading. IRCOBI Conference Proceedings 2017, Antwerp, Belgium.

[5] Mukherjee, S., Zeng, W., Roberts, C., Caudillo, A., Forman, J., Panzer, M. (2022) Validation of small female foot and ankle finite element model under shod automotive loading environment. IRCOBI Conference Proceedings 2022, Porto, Portugal.

[6] Forman, J., Crandall, J., Roberts, C. (2017) Lower Leg Biofidelity and Injury Risk Assessment – Biofidelity Corridors for Heel Impact. Final Report. NHTSA Contract No. DTNH2215D00022/0003.

[7] Forman, J., Crandall, J., Roberts, C. (2017) Lower Leg Biofidelity and Injury Risk Assessment – Biofidelity Corridors for Ankle Dorsiflexion. Final Report. NHTSA Contract No. DTNH2215D00022/0003.

[8] Roberts, C., Forman, J., Kerrigan, J. (2018) Injury risk functions for 5th percentile females: ankle inversion and eversion. IRCOBI Conference Proceedings 2018, Athens, Greece.

[9] Nie, B., Panzer, M. B., Mane, A., Mait, A. R., Donlon, J. P., Forman, J. L., Kent, R. W. (2017) Determination of the in situ mechanical behavior of ankle ligaments. Journal of the mechanical behavior of biomedical materials, 65: pp.502–512.

[10] Kulkarni, S., Roberts, C., Foltz, P., & Forman, J. (2020) Biofidelity of THOR 5th Percentile Female ATD in Ankle Eversion and Inversion. SAE Technical Paper, 2(2020-01-0528).

[11] Noss, J., Donlon, J. P., Hallman, J., Carpenter, R., Forman, J. (2024) A Proposed Method for Determination of Distal Tibia Fracture Tolerance for Prediction of Ankle Injuries. SAE Technical Paper, 2024-01-2488.